PNAS RESEARCH ARTICLE | DEVELOPMENTAL BIOLOGY

Acetyl-CoA-mediated autoacetylation of fatty acid synthase as a metabolic switch of de novo lipogenesis in *Drosophila*

Ting Miao[a], Jinoh Kim[a], Ping Kang[a], Hideji Fujiwara[b], Fong-Fu Hsu[b], and Hua Bai[a,1]

Edited by Utpal Banerjee, University of California Los Angeles, Los Angeles, CA; received July 16, 2022; accepted October 31, 2022

De novo lipogenesis is a highly regulated metabolic process, which is known to be activated through transcriptional regulation of lipogenic genes, including fatty acid synthase (FASN). Unexpectedly, we find that the expression of FASN protein remains unchanged during *Drosophila* larval development from the second to the third instar larval stages (L2 to L3) when lipogenesis is hyperactive. Instead, acetylation of FASN is significantly upregulated in fast-growing larvae. We further show that lysine K813 residue is highly acetylated in developing larvae, and its acetylation is required for elevated FASN activity, body fat accumulation, and normal development. Intriguingly, K813 is autoacetylated by acetyl-CoA (AcCoA) in a dosage-dependent manner independent of acetyltransferases. Mechanistically, the autoacetylation of K813 is mediated by a novel P-loop-like motif (N-xx-G-x-A). Lastly, we find that K813 is deacetylated by Sirt1, which brings FASN activity to baseline level. In summary, this work uncovers a previously unappreciated role of FASN acetylation in developmental lipogenesis and a novel mechanism for protein autoacetylation, through which *Drosophila* larvae control metabolic homeostasis by linking AcCoA, lysine acetylation, and de novo lipogenesis.

de novo lipogenesis | FASN | autoacetylation | acetyl-CoA | animal development

Significance

Metabolic homeostasis plays a vital role in animal growth. Here, we show that acetylation of fatty acid synthase (FASN) contributes to de novolipogenesis during fly development. Although acetylation of most proteins is catalyzed by various acetyltransferases (KATs), we unexpectedly find that acetylation of FASN at K813 residue does not require the participation of any known KATs, while it is directly regulated by abundance of acetyl-CoA via a conserved motif nearby K813. The ability to sense and respond to nutrient availability is essential for organisms to maintain metabolic homeostasis and sustain life. Our work highlights a novel metabolite sensing mechanism and a self-regulatory system in the control of metabolic homeostasis through acetyl-CoA-mediated autoacetylation.

De novo lipogenesis (DNL) is a complex yet highly regulated metabolic process which converts excess carbohydrates into fatty acids that are then esterified to storage triglyceride (TAG) (1, 2). Abnormal upregulation of DNL is a vital contributor to increased fat mass in the pathogenesis of various metabolic disorders involving non-alcoholic fatty liver disease and diabetes and in the progression of tumors (3–7). DNL is known to be transcriptionally regulated via sterol regulatory element-binding protein 1 (SREBP1c) and carbohydrate-responsive element-binding protein (ChREBP) in response to metabolic and hormonal cues (8–10). However, it has been recently proposed that allosteric regulation and post-translational modifications (PTMs) are indispensable to control metabolic flux since the timescale of the gene expression is too long to balance the quick turnover of metabolites (11). Lipid anabolism is active during *Drosophila* larval development, and the excessive TAG storage in larvae is an essential reservoir for surviving from starvation in the post-feeding pupa stage of metamorphosis (12, 13). The fatty acids stockpiled in TAG are either derived from the diet or DNL (3, 4, 14, 15). Regulated by hormonal and transcriptional programs, the mRNA expressions of multiple enzymes in DNL pathways, including acetyl-CoA carboxylase (ACC) and fatty acid synthase (FASN), correlate with the dynamic changes in TAG levels in fly embryonic and larval development (12, 13, 16, 17). However, whether PTMs are involved in the regulation of developmental DNL is poorly studied.

Lysine acetylation has recently risen as a novel player that links metabolites [e.g., acetyl coenzyme A (acetyl-CoA)], cell signaling, and gene regulation (18, 19). Previous acetylome studies found that almost all metabolic enzymes are acetylated (20–22), including FASN (23–25). FASN, an essential cytosolic enzyme in DNL pathway, catalyzes the biosynthesis of saturated fatty acids from acetyl-CoA (AcCoA) and malonyl coenzyme A (malonyl-CoA) (26). Recently, FASN has emerged as a novel therapeutic target for the treatment of obesity, diabetes, fatty liver diseases, and cancers (6, 27–29). Although FASN is known to be regulated through SREBP1-mediated transcriptional activation (8–10), several conflicting results show little correlation between FASN expression and its enzymatic activity (23, 24, 30–32). These findings suggest a possible involvement of PTMs in the regulation of FASN function. Phosphorylation and acetylation have been proposed as alternative mechanisms of FASN regulation (23–25). Nevertheless, how PTMs regulate FASN activity and lipogenesis remains largely unknown.

Although protein acetylation is mainly catalyzed by lysine acetyltransferases (KATs), it has been recently reported that acetylation also arises from a nonenzymatic reaction with AcCoA in eukaryotes (33–35). AcCoA is the acetyl donor for protein acetylation and is a reactive metabolic intermediate involved in various metabolic pathways (36). The levels of AcCoA fluctuate in response to both intracellular and extracellular cues (e.g., growth signals and

Author contributions: T.M. and H.B. designed research; T.M., J.K., P.K., H.F., F.-F.H., and H.B. performed research; T.M. and H.B. analyzed data; and T.M. and H.B. wrote the paper.

The authors declare no competing interest.

This article is a PNAS Direct Submission.

[1]To whom correspondence may be addressed. Email: hbai@iastate.edu.

This article contains supporting information online at https://www.pnas.org/lookup/suppl/doi:10.1073/pnas.2212220119/-/DCSupplemental.

Published December 2, 2022.

nutrient conditions), which consequently impacts chromatin modifications and transcriptional reprogramming (36, 37). Previously, it was thought that nonenzymatic acetylation only occurs to mitochondria proteins, as high concentrations of AcCoA and alkaline environment inside mitochondrial matrix favor lysine nucleophilic attack on the carbonyl carbon of AcCoA (34). In recent years, the capability of enzyme-independent acetylation of cytosolic proteins was also determined (33, 38). Yet, the mechanism of nonenzymatic acetylation, especially of cytosolic proteins, remains elusive.

Here, we show that the expression of *Drosophila* FASN (dFASN or FASN1) protein remains unchanged during larval development, the stages when lipogenesis is hyperactive. In contrast, acetylation of dFASN at K813 is significantly induced in response to increased cellular AcCoA levels, which elevates dFASN enzymatic activity and lipogenesis in fast-growing larvae. Strikingly, we find that acetylation of K813 is controlled through a unique KAT-independent mechanism that involves a novel motif "N-xx-G-x-A." In summary, our findings uncover a novel AcCoA-mediated self-regulatory module that regulates developmental lipogenesis via autoacetylation of dFASN.

Results

Acetylation Modification of dFASN, but Not Protein Expression, Is Positively Correlated with DNL during *Drosophila* Larval Development. *Drosophila* development takes around 10 d, with the embryonic stage, three larval stages (L1, L2, and L3 instar larval stages), non-feeding wandering larval stage, and pupal stage. Anabolic pathways, including DNL, are highly activated during larval growth, and *Drosophila* larvae undergo more than a 200-fold increase in body mass in less than 4 d (39, 40). Consistent with that, TAG storage dramatically increased during larval development, especially at the L3 stage (Fig. 1*A*).

Upregulation of DNL is a significant contributor to increased fat mass (3, 4). We found that enzymatic activity of the lipogenic enzyme dFASN was upregulated with larval growth and was highly correlated with TAG levels (Fig. 1*B*). The activation of FASN is mainly through upregulation of transcription and translation (8–10). Although the mRNA expression was slightly induced at L3 stage (96 h after egg laying, 96 h AEL) (Fig. 1*C*), we surprisingly found that the protein expression of dFASN remained unchanged from 48 to 96 h AEL (Fig. 1 *D* and *E*). These results were consistent with previously published developmental RNA-seq and proteomics analysis (*SI Appendix*, Fig. S1 *L* and *M*), although both dFASN mRNA and protein expression were highly correlated with TAG accumulation when the entire development stages, from embryo to pupa, were considered (*SI Appendix*, Fig. S1 *L* and *M*). These data suggest that PTMs might be involved in dFASN activation and fine-tune dFASN function at the fast-growing L3 stage.

To investigate the role of PTMs in regulating dFASN function, we generated a knock-in fly line through CRISPR/Cas9-mediated homology-directed repair (HDR) technique, in which a 3xFlag tag was precisely inserted at the 3′-end of the dFASN coding

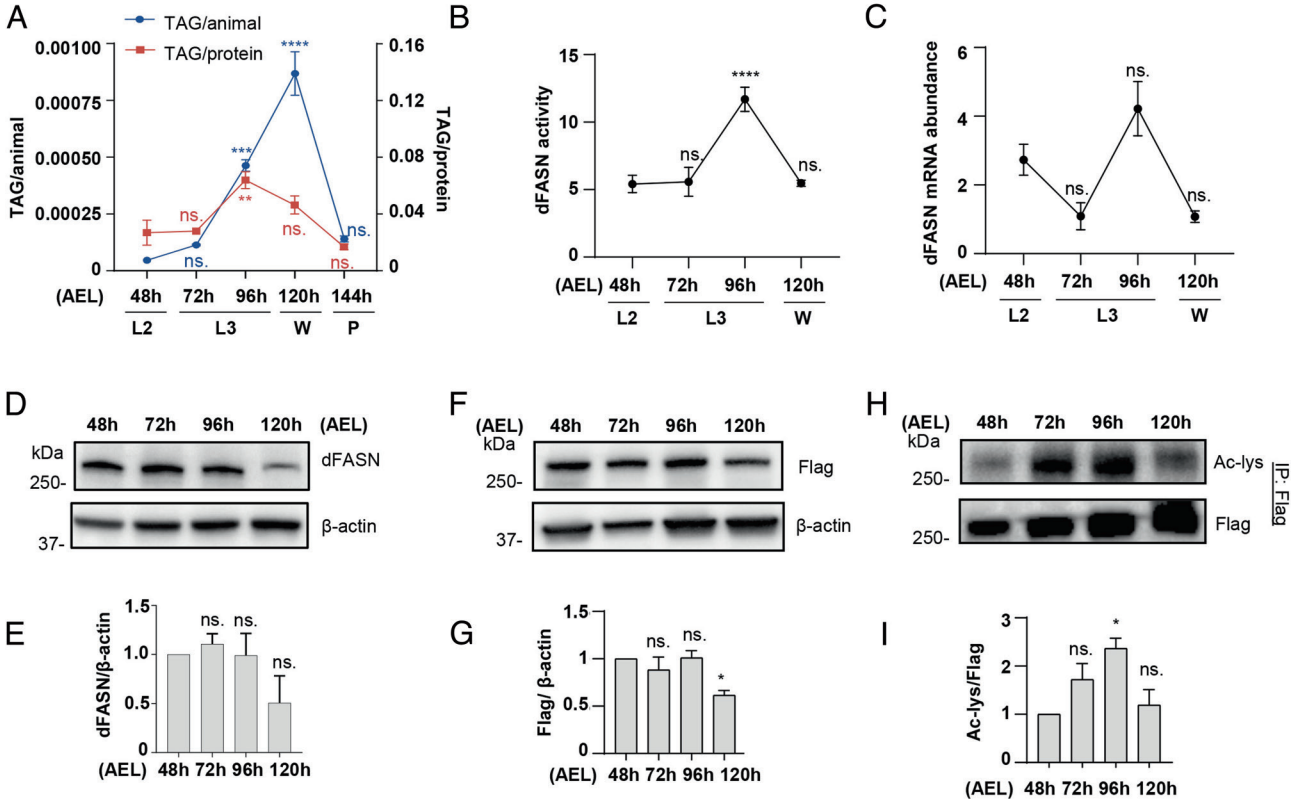

Fig. 1. Acetylation of dFASN, but not protein expression, is positively correlated with de novo lipogenesis during *Drosophila* larval development. (*A*) Stage-specific triglyceride (TAG) level in *Drosophila* larvae. TAG (mg) was normalized against total protein amount or number of larvae (or pupa). AEL: after egg laying. L2: 2nd instar larvae. L3: 3rd instar larvae. W: wandering larvae. P: pupae. (*B*) Stage-specific dFASN enzymatic activity. dFASN activity was determined by oxidized NADPH per minute per mg of total protein. (*C*) Stage-specific dFASN mRNA abundance analyzed by qRT-PCR. (*D* and *E*) Stage-specific dFASN protein expression analyzed by western blotting with an antibody recognizing dFASN (anti-dFASN). (*F* and *G*) Stage-specific endogenous FASN-Flag protein expression analyzed by western blotting with anti-Flag antibody. (*H* and *I*) Stage-specific dFASN acetylation. dFASN-Flag was immunoprecipitated from *FASN*^{Flag} larvae followed by western blotting analyses. dFASN acetylation was detected by anti-acetylated-lysine antibody (anti-Ac-lys). Values shown are mean SD; ns. $P > 0.5$; *$P < 0.05$; **$P < 0.01$; ***$P < 0.001$; and ****$P < 0.0001$. One-way ANOVA (vs. 48 h).

region (*SI Appendix*, Fig. S1 *A–E*). The knock-in lines are homozygous viable, fertile, and exhibit normal larval development and body fat accumulation (*SI Appendix*, Fig. S1 *F–H*). Similar to the above western blot analysis using dFASN antibodies (Fig. 1 *D* and *E*), the levels of endogenous dFASN proteins from 3xFlag knock-in flies were not changed from L2 to L3, either (Fig. 1 *F* and *G*). However, dFASN protein expression was decreased at 120 h AEL (wandering stage) (Fig. 1 *D–G*), which may also contribute to the lower levels of dFASN activity.

Phosphorylation and acetylation are two known modifications of FASN identified from previous studies (23–25). To characterize these two modifications during larval development, we immunoprecipitated endogenous dFASN from the knock-in fly line $FASN^{Flag}$ with an anti-Flag antibody followed by western blot analysis. Intriguingly, the acetylation levels of dFASN were highly correlated with its enzymatic activity, with a peak at 96 h AEL (Fig. 1 *H* and *I*). In comparison, phosphorylation of dFASN did not change from 48 to 96 h AEL (*SI Appendix*, Fig. S1*I*). To exclude the possibility that increased dFASN acetylation at L3 larvae is due to global changes in acetylome, we measured histone acetylation marks in developing larvae. Interestingly, none of the histone acetylation marks changed significantly throughout larval development (*SI Appendix*, Fig. S1*J*). We also checked stage-specific global protein acetylation and found that not all protein acetylation increased at L3 stage (*SI Appendix*, Fig. S1*K*). These results suggest that upregulated dFASN acetylation is not due to changes in global acetylation. Taken together, our results indicate acetylation of dFASN, instead of transcription and translation, is the primary regulatory mechanism for accelerated DNL in fast-growing L3 larvae.

K813 Is a Crucial Acetylated Lysine for DNL, Body Fat Accumulation, and Normal *Drosophila* Development. To identify the acetylated lysine sites of dFASN, we carried out a proteomic analysis with immunoprecipitated dFASN from $FASN^{Flag}$ Flies. Eight lysine residues distributed on four different domains of dFASN were identified (*SI Appendix*, Fig. S2*A*). When comparing these lysine sites with previous acetylome studies, we found that K813 and K926 were the most frequently acetylated residues, and both sites are evolutionarily conserved (*SI Appendix*, Fig. S2 *B* and *C*).

We next explored the functional role of acetylated K813 and K926 in developmental lipogenesis with two acetylation-deficient mutants (Lys to Arg substitution), $FASNK^{813R}$ and $FASNK^{926R}$ (*SI Appendix*, Figs. S2*D* and S3 *A–D*). Remarkably, $FASN^{K813R}$ mutants, but not $FASN^{K926R}$, showed decreased dFASN enzymatic activity and body fat accumulation at 96 h AEL (Fig. 2 *A* and *B*). When examining the TAG levels throughout developmental stages, we found that $FASN^{K813R}$ mutants exhibited lower TAG levels at almost all stages (Fig. 2*C*). The protein expression of dFASN in $FASN^{K813R}$ mutants was not affected (*SI Appendix*, Fig. S3 *E* and *F*), suggesting that the reduced dFASN activity and TAG levels did not result from decreased dFASN protein level. In addition, although dFASN activity is impaired in $FASN^{K813R}$, its enzyme function was not destroyed, and the mutants can still develop into viable pupae and adults. While in contrast, dFASN knockout mutants are homozygous lethal (*SI Appendix*, Fig. S3*D*). Therefore, we hypothesize that acetylation at K813 fine-tunes dFASN activity and lipogenesis during larval development.

Dysregulated fatty acid biosynthesis impairs larval growth and development (41). Consistently, we found that pupariation of $FASN^{K813R}$ mutants was significantly delayed, while $FASN^{K926R}$ exhibited normal development (Fig. 2*D*). Sufficient larval-derived body fat is required for the development of adult tissue at the pupal stage, and insufficient lipid accumulation in larval stages may cause growth deficiency (42). Indeed, the body weight of $FASN^{K813R}$ adults was significantly decreased (*SI Appendix*, Fig. S3*G*). Given that the acetylation of K813, not K926, is required for the elevated dFASN activity, increased fat accumulation, and normal larval development, we speculate that K813 acetylation may be positively correlated with dFASN activity. As predicted, the acetylation of K813 significantly increased at 96 h AEL when tested with a newly generated antibody specific to acetylated K813 (acK813) (Fig. 2 *E* and *F* and *SI Appendix*, Fig. S2*E*).

Eukaryotic FASN is a multifunctional protein containing seven activity domains (43). K813 is localized at the malonyl/acetyltransferase (MAT) domain where substrates AcCoA (initiation primer) and malonyl-CoA (MalCoA) (chain extender) are bound (*SI Appendix*, Fig. S2 *A* and *B*) (26). When examining the crystal structure of MAT domains of dFASN and human FASN (hFASN), we found that K673 of hFASN (homolog of dFASN K813) was at the substrate docking pocket of the MAT domain. The predicted structure *of Drosophila* protein revealed a similar localization of K813 as that of hFASN K673 (*SI Appendix*, Fig. S2*F*).

The proximity of K813 to the substrate docking pocket of the MAT domain hints us to test whether acetylation of K813 modulates dFASN catalytic activity upon MalCoA, the main substrates of MAT domain. We measured the activity of dFASN from 48 and 96 h AEL larvae by incubating protein lysates with different concentrations of MalCoA (Fig. 2*G*). Although dFASN activity of both groups increased upon high MalCoA concentration, dFASN from 96 h AEL is more sensitive to the change of MalCoA levels. The activity of dFASN from the two larval stages was similar at low MalCoA concentrations (<60 μM), whereas dFASN activity from 96 h AEL larvae was significantly higher than that of 48 h AEL upon high MalCoA concentrations (60 to 120 μM). Since dFASN protein expressions were similar between the two stages (Fig. 1 *D–F*), we speculated that the alteration in MalCoA-dependent dFASN activity may be caused by acetylation. Additionally, substrate-excess inhibition was observed under high MalCoA dosages (120 to 200 μM) in both groups, consistent with previous kinetics studies on yeast FASN (44). Notably, the measurements of MalCoA in mammalian tissues or flies are generally in the low micromolar range (45, 46). Here a higher concentration of MalCoA used in the activity assays was to maintain a similar amount of MalCoA per FASN protein as seen in the normal physiological conditions.

Next, we expressed recombinant dFASN proteins, which were then used for steady-state kinetics evaluation (Fig. 2*H* and *SI Appendix*, Fig. S3*H*). The recombinant dFASN proteins with K813R substitution showed ~30% reduction of the maximum rate of reaction ($V_{max,\ Malonyl\text{-}CoA}$) compared to wild-type (WT). Consistent with results in Fig. 2*G*, WT proteins exhibited higher activity than K813R mutants upon higher MalCoA concentrations (50 to 200 μM), but not upon low MalCoA concentrations (<50 μM). These results showed that interfering with the acetylation of K813 alters the kinetics properties of dFASN. Steady-state kinetics over AcCoA was also evaluated and there was no difference between WT and K813R mutants (*SI Appendix*, Fig. S3*I*).

Taken together, our findings show that K813 localizes at the substrate docking pocket of the MAT domain, and acetylation of K813 may alter the conformation of the docking pocket to enhance enzyme activity at high substrate concentrations. Here, we propose a fine-tune mechanism of dFASN regulation in which acetylation of K813 modulates dFASN catalytic activity and lipogenesis in response to fluctuated substrate availability during larval development.

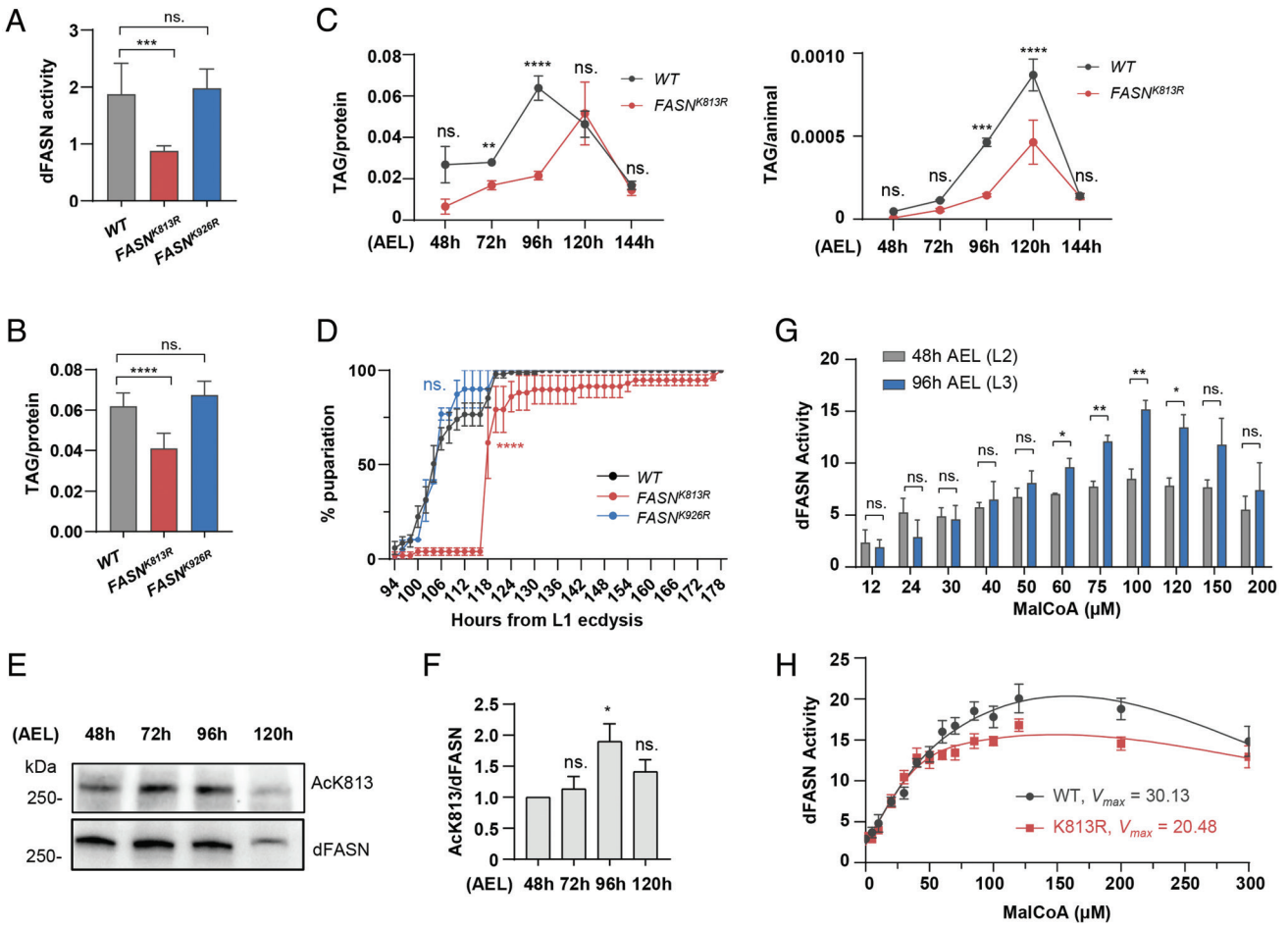

Fig. 2. K813 is a crucial acetylated lysine for de novo lipogenesis, body fat accumulation, and normal *Drosophila* development. (*A*) dFASN enzymatic activity of *WT* (yw^R), $FASN^{K813R}$, and $FASN^{K926R}$ at L3 stage. dFASN activity was determined by oxidized NADPH per minute per mg of protein. (*B*) TAG level of *WT* (yw^R), $FASN^{K813R}$, and $FASN^{K926R}$ at L3 stage. TAG (mg) was normalized against total protein amount (mg) (*Left*) and number of larva (or pupa). (*C*) Stage-specific TAG level of *WT* (yw^R) and $FASN^{K813R}$. TAG (mg) was normalized against total protein amount (mg). (*D*) Developmental timing of *WT* (yw^R), $FASN^{K813R}$, and $FASN^{K926R}$. Number of pupariation was counted every 2 to 4 h. (*E* and *F*) Site-specific acetylation at K813 in larval development stages determined by western blotting analyses. Acetylation of K813 was measured by an antibody specifically recognizing acetylated K813 (anti-AcK813). (*G*) Malonyl-CoA (MalCoA)-dependent dFASN activity at L2 and L3. (*H*) Steady-state kinetics evaluation of WT and K813R recombinant dFASN upon malonyl-CoA. Values shown are mean SD; ns. $P > 0.5$; *$P < 0.05$; **$P < 0.01$; ***$P < 0.001$; and ****$P < 0.0001$. *A* and *B*: One-way ANOVA (vs. yw^R); *C*: Multiple *t* test; *D*: Log-rank test (vs. yw^R); *F*: One-way ANOVA (vs. 48 h); *G*: *t*-test; *H*: Michaelis–Menten analysis.

K813 Is Autoacetylated by AcCoA and Is Regulated by Intracellular AcCoA Flux In Vivo. The unique pattern of dFASN acetylation indicates that it is tightly regulated during *Drosophila* development. We next asked how acetylation of dFASN, especially K813, is regulated. Proteins are primarily acetylated and deacetylated by acetyltransferases (KATs) and deacetylases (KDACs), respectively (47). To identify the KAT that regulates dFASN acetylation in developing larvae, we first checked the mRNA expression of *Drosophila* KATs in previous transcriptomic analysis (*SI Appendix*, Fig. S4 *A* and *B*). Interestingly, none of the KATs showed upregulation in L3 stage when dFASN acetylation is elevated. Next, a genetic screen was performed to identify KATs that are involved in TAG accumulation (*SI Appendix*, Fig. S4*C*). Loss-of-function mutations of Gcn5, Tip60, Chm, and Mof exhibited elevated TAG levels, while Elp3 mutants showed reduced TAG at L3 stage, suggesting that Epl3 may be a positive regulator for lipogenesis and potentially dFASN acetylation. Lastly, we overexpressed the KATs in *Drosophila* Kc167 cells and measured the acetylation level of K813 (*SI Appendix*, Fig. S4 *D* and *E*). The five KATs that were shown to regulate TAG accumulation were cloned to expression vectors. Unexpectedly, ectopic expression of all five KATs failed to induce acetylation of dFASN at K813. These data suggest that acetylation of K813 might be regulated by an unknown KAT, or through a unique KAT-independent mechanism.

Except being enzymatically catalyzed by KATs, lysine acetylation also arises from a nonenzymatic reaction with AcCoA. Interestingly, nonenzymatic acylation of FASN was observed in a recent global nonenzymatic acylation screen (38). However, no follow-up validation was performed to confirm if FASN is nonenzymatically modified by either AcCoA or other acyl-CoAs. To explore the possibility that dFASN acetylation is regulated through a nonenzymatic mechanism, we measured the acetylation of dFASN in vitro by incubating recombinant dFASN with 5 to 20 μM of acetyl-CoA (AcCoA), the dosages close to actual cytosolic AcCoA levels (34). Intriguingly, dFASN was rapidly acetylated by as few as 5 μM of AcCoA in 1 h (Fig. 3 *A* and *B*). Consistent with the idea that nonenzymatic acetylation favors alkaline conditions (34, 48), the acetylation levels of recombinant dFASN were higher at pH8.0 than at pH7.0. In contrast, bovine serum albumin (BSA) showed no autoacetylation, even when the proteins were incubated with 200 μM of AcCoA for 6 h (Fig. 3 *C* and *D*). More strikingly, autoacetylation of dFASN was largely blocked by K813R substitution (Fig. 3*E*), suggesting that K813 is the primary residue of

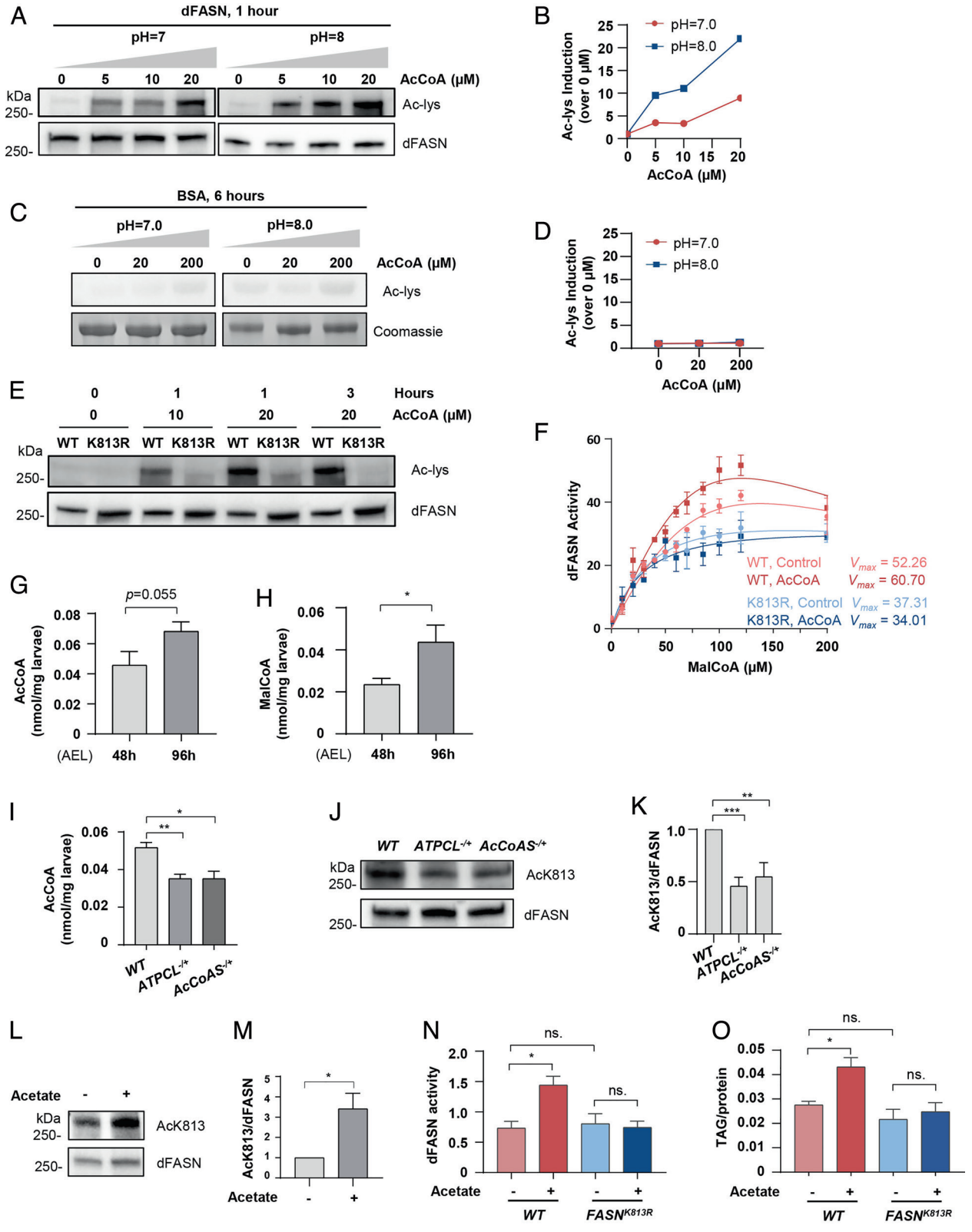

Fig. 3. K813 is autoacetylated by acetyl-CoA and is regulated by intracellular acetyl-CoA flux in vivo. (*A* and *B*) Acetylation of dFASN by acetyl-CoA (AcCoA). Recombinant dFASN was incubated with 0, 5, 10, or 20 μM of AcCoA at pH7.0 or pH8.0 for 1 h prior to western blotting analyses with anti-Ac-lys. Folds of induction over 0 μM of AcCoA treatment were shown in (*B*). (*C* and *D*) Acetylation of BSA by AcCoA treatment. BSA was incubated with 0, 20, or 200 μM of AcCoA at pH7.0 or pH8.0 for 6 h prior to western blotting analyses with anti-Ac-lys. Folds of induction over 0 μM of AcCoA treatment were shown in (*D*). (*E*) Acetylation of WT or K813R dFASN by AcCoA treatment. WT or K813R recombinant dFASN was incubated with 0, 10, or 20 μM of AcCoA at pH8.0 for 1 h or 3 h prior to western blotting analyses. (*F*) Steady-state kinetics evaluation of WT and K813R of recombinant dFASN post-AcCoA treatment. WT or K813R recombinant dFASN were incubated with 20 μM of AcCoA at pH7.0 for 0 or 1 h before activity assay. (*G* and *H*) Intracellular AcCoA and malonyl-CoA (MalCoA) levels of developing *Drosophila* larvae. Figures showed folds of induction over 48 h AEL. (*I*) Intracellular AcCoA levels of *WT* (yw^R), $ATPCL^{-/+}$, and $AcCoAS^{-/+}$. (*J* and *K*) Acetylation of K813 in *WT* (yw^R), $ATPCL^{-/+}$, and $AcCoAS^{-/+}$ at L3 larval stage. (*L* and *M*) Acetylation of K813 of *ywR* L3 larvae supplemented with acetate determined by western blotting analyses with anti-AcK813. (*N*) dFASN enzymatic activity of *ywR* (*WT*) and $FASN^{K813R}$ L3 larvae supplemented with acetate. dFASN activity was determined by oxidated NADPH per minute per mg of protein. (*O*) TAG level in *ywR* (*WT*) and $FASN^{K813R}$ L3 larvae supplemented with acetate. TAG (mg) was normalized against total protein amount (mg). Values shown are mean SD; ns. $P > 0.5$; *$P < 0.05$; **$P < 0.01$; and ***$P < 0.001$. *F*: Michaelis–Menten analysis; *G*, *H*, *I* and *M*: *t* test; *K*: One-way ANOVA (vs. *WT*); *N* and *O*: One-way ANOVA (multiple comparisons).

dFASN that could be autoacetylated. Moreover, recombinant dFASN pre-incubated with AcCoA showed 16% increases in $V_{max,\ Malonyl\text{-}CoA}$, while $V_{max,\ Malonyl\text{-}CoA}$ of K813R mutant protein was not altered by AcCoA treatment, suggesting that AcCoA-mediated autoacetylation of K813 modulates dFASN activity (Fig. 3*F*). Consistent with results in Fig. 2*H*, the activity of WT proteins without AcCoA pre-incubation was similar to that of K813R mutants upon low MalCoA concentrations (<60 μM), while the AcCoA-treated WT proteins exhibited a higher activity than the other groups (*SI Appendix*, Fig. S3*J*).

Our observations on dFASN autoacetylation at pH7.0 upon low concentrations of AcCoA in a dosage-dependent manner suggest that endogenous dFASN proteins may be autoacetylated in vivo, and an autoregulatory mechanism might be used by developing larvae to fine-tune dFASN acetylation and enzymatic activity in response to fluctuating cytosolic AcCoA levels. To explore this idea, we first measured larvae AcCoA levels by LC-MS/MS and found that AcCoA increased at 96 h AEL compared to 48 h AEL (Fig. 3*G*). ATP citrate lyase (ATPCL) and acetyl coenzyme A synthase (AcCoAS) are two main contributors to the cytosolic AcCoA pool (36). mRNA expressions of the two genes are both upregulated at L3 stage (*SI Appendix*, Fig. S4*F*), consistent with our LC-MS/MS results. MalCoA was also elevated at 96 h AEL (Fig. 3*H*), supporting our hypothesis that K813 acetylation fine-tunes dFASN activity in response to fluctuated substrate MalCoA availability during larval development.

Next, to determine whether AcCoA-producing enzymes regulate dFASN acetylation in vivo, we measured AcCoA levels and acetylation of K813 in ATPCL and AcCoAS loss-of-function mutants. AcCoA was significantly dropped in $ATPCL^{[01466]/+}$ *and* $AcCoAS^{[MI12066]/+}$ mutants at 96 h AEL, and K813 acetylation was reduced 50% in both mutants (Fig. 3 *I*–*K*). Acetate supplementation is commonly used to elevate cytosolic AcCoA and restore compromised histone acetylation (49–51). When manipulating cytosolic AcCoA in developing larvae by acetate feeding, we found that acetylation of dFASN at K813 in early L3 larvae was significantly increased (Fig. 3 *L* and *M*). These data suggest that K813 acetylation is sensitive to cytosolic AcCoA flux. Furthermore, both dFASN activity and TAG accumulation of *WT* early L3 larvae were increased under acetate feeding, while the elevations were blocked in $FASN^{K813R}$ mutants (Fig. 3 *N* and *O*). These results demonstrate that autoacetylation of dFASN in response to AcCoA flux plays a vital regulatory role in fly developmental lipogenesis.

N-xx-G-x-A Motif Is Required for Autoacetylation of K813. It has been shown that mitochondrial proteins can be acetylated when incubated with high dosages of AcCoA (200 μM to 1.5 mM) in alkaline buffer (pH = 8.0) for over 3 h (34, 52). However, our results revealed that dFASN could be acetylated under a much tougher condition (Fig. 3 *A* and *B*), suggesting that an efficient and unique mechanism is involved in AcCoA-mediated dFASN autoacetylation.

To uncover the mechanism underlying dFASN autoacetylation, we expressed recombinant KS-MAT didomain of dFASN using in *Escherichia coli* BL21 (DE3) expression system (53) (*SI Appendix*, Fig. S4*G*). For system validation, we incubated recombinant KS-MAT with different amounts of AcCoA for 1 h and checked the acetylation of K813 by western blot analysis. Same as recombinant dFASN produced by the Bac-to-Bac expression system, recombinant KS-MAT was also autoacetylated by AcCoA in a dosage-dependent manner, although the induction of autoacetylation was not as strong as the full-length dFASN (Fig. 4*A*). Acetylation of recombinant KS-MAT under 20 μM AcCoA treatment was not prominent, which could be due to the differences in protein folding between prokaryotic and eukaryotic expression systems. Therefore, 200 μM of AcCoA was applied for the following analyses. We further confirmed that K813R substitution blocked AcCoA-mediated autoacetylation of recombinant KS-MAT proteins (Fig. 4*B*). In contrast, K926R substitution did not affect autoacetylation of KS-MAT by AcCoA treatment (Fig. 4*B*).

Previous studies found that high stoichiometry acetylation of lysine is associated with neighboring cysteine (54), and peptides containing a cysteine near a lysine residue exhibit increased nonenzymatic acetylation in vitro (52). However, we could not locate any cysteine near K813 residue from the primary and tertiary structure of dFASN. Since dFASN can be rapidly acetylated by low concentration of AcCoA at the neutral condition, we wonder whether dFASN has adapted some features of KATs to facility its autoacetylation. Intriguingly, we found a highly conserved motif (N-xx-G-x-A, where x denotes any amino acid), two amino acids away from K813, which resembles the signature P-loop sequence (R/Q-xx-G-x-A/G) of KATs (55). The alignment of the FASN amino acid sequences from a variety of animal species revealed that the first position of the motif is conditionally conserved (N in invertebrates and R/Q in vertebrates), while the fourth (G) and sixth (A) positions of the motif are highly conserved across all species (Fig. 4*C*).

P-loop is an invariant sequence in KATs motif A for AcCoA recognition and binding, and KATs activity is largely disrupted when mutating any of the three signature residues (56–59). To investigate the role of the N-xx-G-x-A motif in K813 autoacetylation, we expressed three recombinant proteins carrying N816A, G819A, or A821W substitutions (*SI Appendix*, Fig. S4*G*). WT and mutant proteins were incubated with AcCoA followed by western blot analysis (Fig. 4 *D* and *E*). Strikingly, the induction of K813 acetylation was blocked by all single-site mutations, N816A, G819A, and A821W. Since A821 is not a surface residue, to exclude the possibility that the blockage of autoacetylation by A821W mutant is due to the disruption of protein structure, we also tested another substitution, A821M. Similarly, recombinant proteins with A821M substitution showed no induction of K813 acetylation by AcCoA. In addition, these single-site substitution mutations also blocked total acetylation of KS-MAT recombinant proteins when testing with Ac-lys antibody (Fig. 4*E*). Together, these results demonstrate that N-xx-G-x-A motif is required for autoacetylation of K813.

Sirt1-Mediated Deacetylation of dFASN Regulates Lipogenesis and Developmental Timing in *Drosophila* Larvae. Finally, we examined how K813 is deacetylated. When examining the developmental expression profiles of fly KDACs from HDACs and SIRTs family, we found that the pattern of mRNA expression of *Sirt1* negatively correlates with dFASN acetylation, high at L1 and pupa stage, while low at L3 larval stage (*SI Appendix*, Fig. S5 *A* and *B*). Then, we conducted a genetic screening to examine the role of KDACs in TAG accumulation. Loss-of-function mutations of three sirtuins (Sirt1, Sirt4, and Sirt7) showed elevated TAG levels, suggesting a negative role of these sirtuins in lipogenesis and potentially dFASN acetylation (*SI Appendix*, Fig. S5*C*). Nevertheless, only Sirt1 is localized in the cytoplasm (*SI Appendix*, Fig. S5*A*). Moreover, Sirt1 is a known negative regulator heavily involved in lipid synthesis pathways (60, 61). Altogether, we speculated that Sirt1 might be a promising candidate KDAC deacetylating dFASN.

Next, we ectopically expressed *Sirt1* using daughterless GeneSwitch-Gal4 driver (da-GS-Gal4) at the L3 stage. Remarkably, short-term

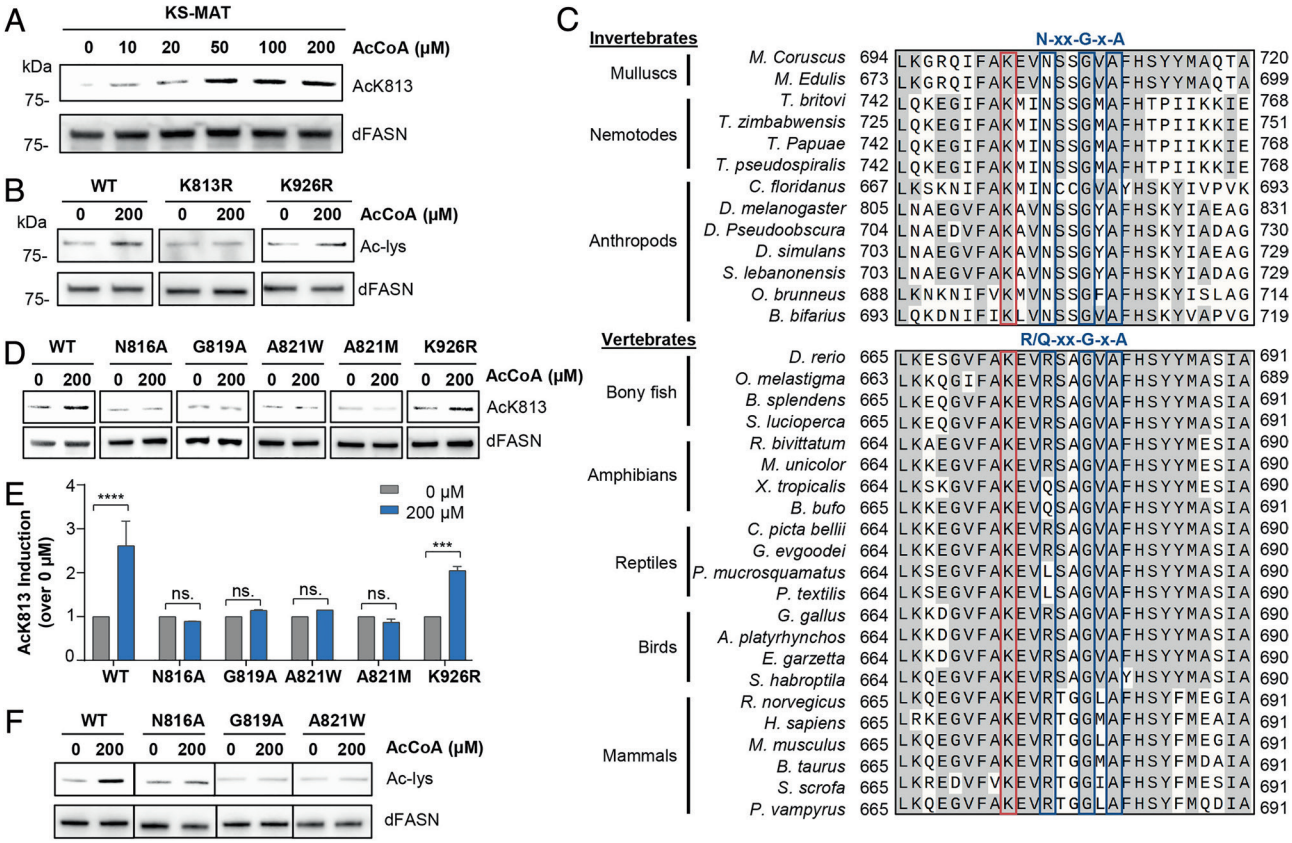

Fig. 4. N-xx-G-x-A motif is required for autoacetylation of K813. (*A*) K813 acetylation of KS-MAT by AcCoA treatment. Recombinant KS-MAT didomain was incubated with 0, 10, 20, 50, 100, and 200 μM of AcCoA at pH8.0 for 1 h or 3 h prior to western blotting analyses with anti-AcK813. (*B*) Total acetylation of WT and mutant KS-MAT by AcCoA treatment. WT, K813R, or K926R recombinant KS-MAT was incubated with 200 μM of AcCoA at pH8.0 for 1 h prior to western blotting analyses with anti-Ac-lys. (*C*) Sequence alignment of MAT domain (the region surrounding acetylated K813) among invertebrate and vertebrate species. Acetylated lysine is highlighted in red. The P-loop-like motif (N-xx-G-x-A in invertebrates or R/Q-xx-G-x-A in vertebrates) is highlighted in blue. (*D* and *E*) AcCoA-mediated K813 acetylation of single-site mutations (N816A. G819A, A821W, A821W, and K926R). WT or mutant KS-MAT recombinant proteins was incubated with 200 μM of AcCoA at pH8.0 for 1 h prior to western blotting analyses with anti-AcK813. (*F*) Total acetylation of single-site mutations by AcCoA treatment. WT, N816A, G819A, or A821W recombinant KS-MAT was incubated with 200 μM of AcCoA at pH8.0 for 1 h prior to western blotting analyses with anti-Ac-lys. Values shown are mean SD; ns. $P > 0.5$; ***$P < 0.001$; and ****$P < 0.0001$. *G: t* test.

overexpression (1 d) of *Sirt1* removed acetylation at K813 by about 90%. Notably, overexpression of *Sirt1* did not alter dFASN protein expression, although it was reported that the transcription of FASN is indirectly regulated by *Sirt1* through deacetylation of SREBP1c (Fig. 5 *A*–*C*) (62–64). We then showed that Sirt1 interacted with MAT domain of dFASN through a co-immunoprecipitation experiment by co-expressing HA-tagged Sirt1 and Flag-tagged MAT domain in *Drosophila* Kc167 cells (Fig. 5*D*). Furthermore, acetylation of K813 was increased in $Sirt1^{[2A]/+}$ loss-of-function mutants at L3 stage (Fig. 5*D*), which could potentially explain for the elevation of TAG in $Sirt1^{[2A]/+}$ (*SI Appendix*, Fig. S5*C*). Lastly, our in vitro deacetylation assay provided direct evidence that dFASN was deacetylated by Sirt1 (*SI Appendix*, Fig. S5 *D* and *E*). More interestingly, although WT dFASN recombinant protein exhibited higher activity than K813R mutant at 120 μM of MalCoA (Figs. 2*H* and 3*F*), there was no significant difference between the activity of deacetylated WT dFASN and K813R mutant (*SI Appendix*, Fig. S5*F*).

Lastly, to determine whether K813 acetylation is required for Sirt1-mediated lipogenesis, we performed an epistasis analysis by measuring TAG levels of $Sirt1^{[2A]}/FASN^{K813R}$ double mutants (Fig. 5*G*). Intriguingly, the elevated TAG levels in $Sirt1^{[2A]/+}$ were rescued by $FASN^{K813R/+}$ mutants, suggesting that the role of Sirt1 in body fat accumulation is through dFASN deacetylation. Consistently, $Sirt1^{[2A]/+}$ developed faster and showed early pupariation compared to WT flies, which were rescued by $FASN^{K813R/+}$ mutants (Fig. 5*H*). Taken together, these results demonstrate that Sirt1 is the primary deacetylase targeting K813. Acetylation of K813 is required for Sirt1-mediated lipogenesis and larval development.

Discussion

Metabolic homeostasis plays an important role in animal development and growth (65, 66). One novel mechanism underlying the coordination of metabolic homeostasis and growth is the interplay between metabolic intermediates and PTMs (67, 68). In the present study, we uncover a novel role of AcCoA-mediated autoacetylation of dFASN in lipogenesis during *Drosophila* larval development (Fig. 5*I*). On the one hand, AcCoA fuels dFASN as the carbon donor for the growing fatty acid chain. On the other hand, AcCoA, as the acetyl-group donor, directly modulates dFASN enzymatic activity through acetylation of the critical lysine residue K813. Additionally, we surprisingly found that acetylation of dFASN does not require KATs; instead, it is mediated by a conserved P-loop-like motif N-xx-G-x-A neighboring K813. Lastly, we identified Sirt1 as the primary deacetylase for dFASN, which acts as a negative regulatory mechanism.

Acetylation of dFASN at K813 as a Novel Fine-Tune Mechanism for Developmental DNL and Metabolic Homeostasis. TAG levels are tightly controlled during *Drosophila* development, and the

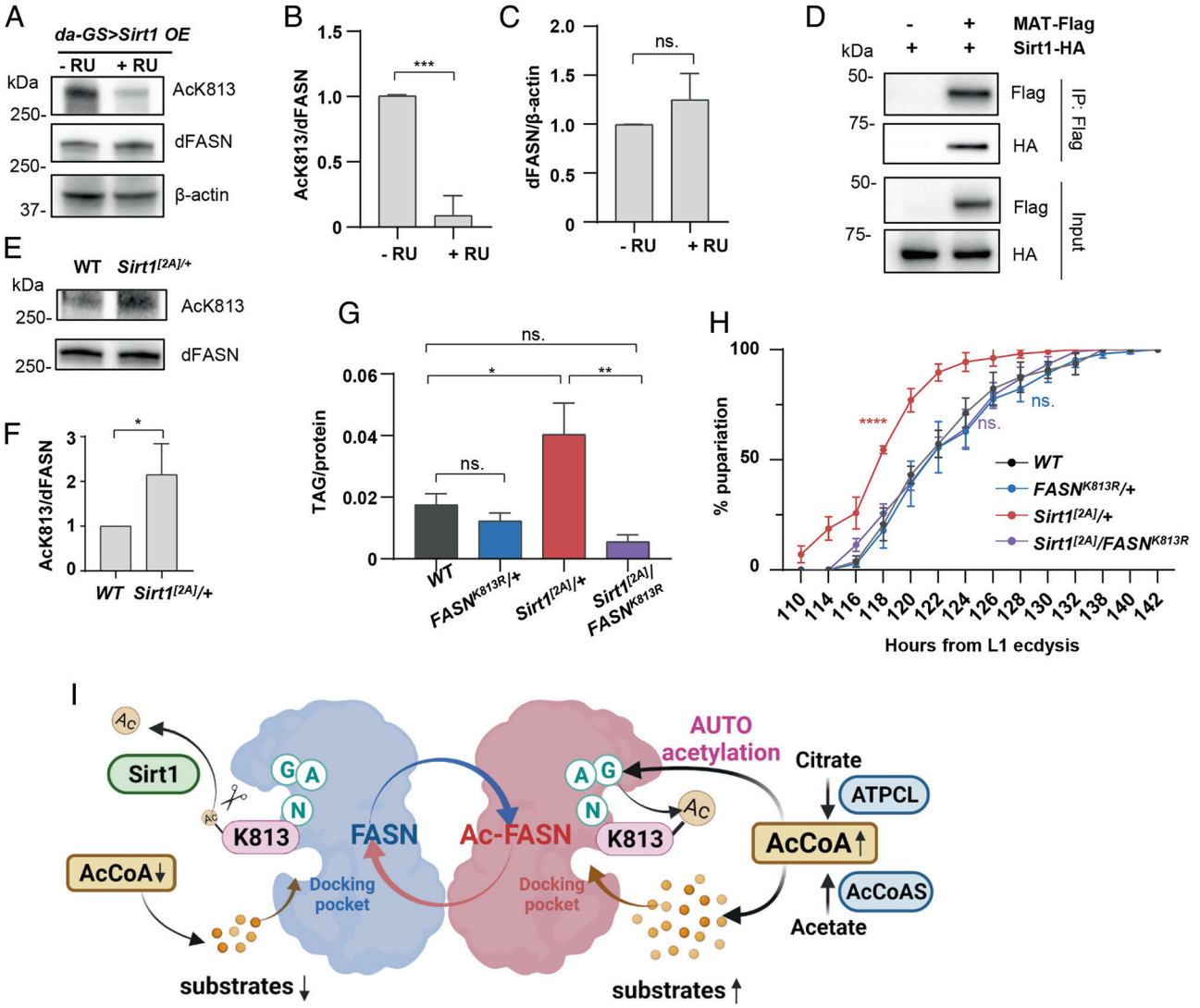

Fig. 5. Sirt1-mediated deacetylation of dFASN1 regulates lipogenesis and developmental timing in *Drosophila* larvae. (*A*, *B*, and *C*) Acetylation of K813 in L3 larvae overexpressing *Sirt1*. Western blotting was performed using anti-AcK813. Daughterless GeneSwitch (GS)-Gal4 driver was used to drive ubiquitous expression of *Sirt1*. The expression was activated by 100 μM of RU468 (+ RU). (*D*) Co-immunoprecipitation of Sirt1 and the MAT domain of dFASN. Kc167 cells were transfected by plasmids encoding Flag-tagged MAT and HA-tagged Sirt1. Interaction between MAT and Sirt1 was determined by western blotting analyses with anti-HA antibodies. (*E* and *F*) Acetylation of K813 in *WT* (yw^R/w^{1118}) and $Sirt1^{[2A]/+}$ larvae. (*G*) TAG levels in $WTFASN^{K813R/+}Sirt1^{[2A]/+}$, and $Sirt1^{[2A]}/FASN^{K813R}$. TAG (mg) was normalized against total protein amount (mg). (*H*) Developmental timing of yw^R/w^{1118}(*WT*), $FASN^{K813R/+}Sirt1^{[2A]/+}$, and $Sirt1^{[2A]}/FASN^{K813R}$. Number of pupariation was counted every 2 to 4 h. (*I*) Working model showing acetyl-CoA-mediated autoacetylation of fatty acid synthase. The model figure was created with BioRender.com. Values shown are mean SD; ns. $P > 0.5$; *$P < 0.05$; **$P < 0.01$; ***$P < 0.001$; and ****$P < 0.0001$. *B*, *C*, and *F*: *t* test; *G*: One-way ANOVA (multiple comparisons); *H*: Log-rank test (vs. *WT*).

massive buildup of TAG storage is a feature of larval growth (12, 13, 17). TAG synthesis is catalyzed by isoenzymes and competes with pathways that consume fatty acids, such as fatty acid oxidation and membrane lipid synthesis (15, 69). During the entire embryonic and larval development, the mRNA expressions of multiple lipogenic enzymes, including *FASN*, correlate with TAG levels (12, 13, 16, 17). Moreover, flies with mutations in *FASN1* and *FASN2* store less TAG in both larval and adult stages of *Drosophila*, suggesting that DNL is a vital contributor to TAG storage throughout development (14).

Under conditions like excess nutrition, growth factor stimulation, obesity, diabetes, fatty liver diseases, or cancer, DNL is significantly elevated, and the mRNA expression of FASN positively correlates with elevated lipogenesis (6, 27–29). However, the protein levels of FASN are rarely characterized. Interestingly, several conflicting results show little correlation between FASN protein expression and its enzymatic activity (23, 24, 30–32). Consistently, we found that the protein levels of dFASN remain unchanged from L2 to L3 and do not match the pattern of its enzymatic activity. In contrast, acetylation of dFASN at lysine K813 is positively associated with dFASN activity, developmental lipogenesis, and TAG accumulation. However, although dFASN level is not upregulated with elevated lipogenesis and TAG accumulation at L3 larvae, it correlates with TAG levels when the entire embryonic and larval development stages are considered. Our findings suggest that despite the well-established transcriptional program controlling the expression of dFASN at different stages of development, lysine acetylation of dFASN plays a crucial role in accelerating dFASN activity and fine-tuning dFASN-mediated lipogenesis in fast-growing L3 animals.

Indeed, our genetic and biochemical analysis further demonstrates that K813R substitution reduces dFASN enzymatic activity and lipogenesis, while AcCoA-mediated acetylation of recombinant dFASN proteins increases its enzyme activity. Although acetylation of FASN has been reported in several previous global acetylome studies, the functional roles of FASN acetylation remain

largely unknown. A recent study investigated the role of FASN acetylation in DNL in human cell culture (25). The study shows that treatment of KDAC inhibitors induces the acetylation of hFASN, promotes FASN degradation, and reduces lipogenesis. However, it remains to be determined whether the regulation of lipogenesis by KDAC inhibition is due to global acetylation, or if it is directly through FASN acetylation. In addition, the functional lysine residues of hFASN that are responsible for altered lipogenesis are not identified. Because of the high conservation between K813 of dFASN and K673 of hFASN, it is possible that K673 is the key lysine residue mediating DNL in human.

Apart from K813, other three lysine residues of dFASN (K926, K1800, and K2466) are highly conserved among animal species, and their homologs are also found to be acetylated in other animal species. Since these lysine residues are located on different domains, it is not hard to imagine that acetylation of each lysine may play distinct roles related to their associated domains. In the present study, we show that acetylation of K813, but not K926, modulates dFASN activity, body fat accumulation, and *Drosophila* developmental timing. It is likely that acetylation of K926 affects other aspects of enzyme properties that are less important for larval development. K813 is at the substrate docking pocket of the MAT domain. This unique localization suggests that acetylation of K813 might introduce conformational changes to the docking site and modulate dFASN catalytic activity in response to substrate availability during larval development.

N-xx-G-x-A Motif as a Novel Mechanism for Rapid Autoacetylation. Another surprising finding from our study is that acetylation of dFASN at K813 does not require a KAT; rather, it is autoacetylated by AcCoA in a dosage-dependent manner. The cytosolic pool of AcCoA increases under feeding or excess nutrient conditions (37). Consistently, our studies reveal that the amount of AcCoA elevates in fast-growing larvae, which could modulate dFASN activity by promoting both the biosynthesis of MalCoA and autoacetylation of K813 for the conformational changes of MalCoA docking pocket.

It was previously thought that only mitochondria proteins were nonenzymatically acetylated since no KATs have been identified in mitochondria. Besides, the high AcCoA concentration and relatively high pH of the mitochondrial matrix facilitate the lysine nucleophilic attack on the carbonyl carbon of AcCoA (34). Recently, KAT-independent acetylation of cytosolic proteins has been reported (33, 38). Yet, the underlying mechanism for nonenzymatic acetylation remains largely unknown. When investigating how dFASN is autoacetylated by AcCoA, we uncover a novel motif N-xx-G-x-A near acetylated K813. Substituting any of the three key amino acids largely blocks AcCoA-mediated dFASN autoacetylation. The N-xx-G-x-A motif resembles the signature P-loop sequence (Q/R-xx-G-x-A/G) of KATs, which is required for AcCoA recognition and binding (55). We predict that the N-xx-G-x-A motif of dFASN performs a similar function as the P-loop of KATs for AcCoA binding. Moreover, the N-xx-G-x-A motif is highly conserved, pointing out a conserved mechanism for autoacetylation of FASN.

In addition to the well-established KATs of the MYST, p300/CBP, and GCN5 families, there are over 15 proteins that have been reported to possess KATs activity, such as CLOCK and Eco1 (70–72). Since FASN may contain an AcCoA binding motif of KATs, it is possible that FASN, particularly MAT domain, possesses KATs activity and acetylates other proteins, especially those in DNL pathways. This possibility may be further explored through acetylome analysis in the future.

In summary, we uncover a previously unappreciated role of FASN acetylation in developmental lipogenesis and a novel mechanism for lysine autoacetylation. Our findings provide new insights into AcCoA-mediated metabolic homeostasis during animal development. In addition, our studies underscore a promising therapeutic strategy to combat metabolic disorders by targeting autoacetylation of FASN.

Materials and Methods

Drosophila. A detailed list of fly strains is provided (*SI Appendix*). *ywR* was used as the control in the TAG measurement, developmental timing, and FASN activity assay, unless otherwise noted in the figure legend. Flag knock-in fly line, dFASN acetylation-deficient fly lines, and knockout fly line (*yw; FASN^{KO}*) were generated by CRISPR/Cas9-mediated HDR by ssODNs (*SI Appendix*). Flies were maintained at 25 °C, 60% relative humidity, and a 12-h light/dark cycle. Adults and larvae were either reared on standard cornmeal and yeast-based food or special diet as described in *SI Appendix*.

Immunoprecipitation. Fly larvae or Kc167 cells were lysed with Pierce™ IP Lysis Buffer supplied with deacetylase inhibitor nicotinamide at 4 °C for 20 min. After the removal of unbroken cells and debris by centrifugation (14,000 rpm/30 min), the soluble fractions were collected and incubated with mouse anti-Flag M2 antibody (1:100) at 4 °C overnight. The next day, the lysate-antigen mixture was incubated with SureBeads™ Protein G Magnetic Beads at 4 °C for 3 h. The magnetic beads were then washed three times with Pierce™ IP Lysis Buffer. Proteins were denatured and eluted from the beads with Laemmli sample buffer at 95 °C for 5 min for later analysis (*SI Appendix*).

Quantification of AcCoA and MalCoA by LC-MS/MS. AcCoA and MalCoA levels were measured by LC-MS/MS as previously described (46). About 300 mg of L2 and L3 larvae were snap-frozen in liquid nitrogen and pulverized into powder with mortar and pestle. 300 μL/100 mg of solvent buffer (5% sulfosalicylic acid containing 50 μM DDT) was added to the sample immediately. Samples were sonicated three times for 10 s on ice, and the supernatant was collected by centrifugation at 14,000 × g for 20 min. Right before LC-MS/MS analysis, 2 μL of ammonia (25%) was added to 98 μL of the sample solutions. LC-MS/MS analysis was performed at W. M. Keck Metabolomics Research Laboratory of Iowa State University and Metabolism Division of Washington University School of Medicine following the method described previously.

Recombinant Protein Expression and Purification. dFASN-pAV5a and dFASN-K813R-pAV5a were utilized to produce dFASN recombinant protein in the Bac-to-Bac protein expression system. The expression and purification methods of recombinant dFASN proteins were adapted from a previous study (73) (*SI Appendix*). KS-MAT recombinant proteins were expressed in *E. coli* BL21 (DE3) cells with WT or mutant plasmid constructs (53, 74) (*SI Appendix*).

In Vitro Acetylation Assay. AcCoA was diluted to different concentrations with assay buffer containing 20 mM Tris-HCl (pH7.0 or 8.0), 500 mM NaCl. Recombinant proteins and AcCoA were mixed in assay buffer to a final volume of 40 μL. The reactions were incubated in a water bath at 37 °C for 1 h or 3 h. BSA was dissolved in assay buffer (pH7.0 or pH8.0) and then incubated with AcCoA at the same condition for 6 h. The reactions were terminated by adding Laemmli sample buffer and heat-shock at 95 °C for 5 min. Acetylation was analyzed by western blotting with acetylated antibodies.

Kinetics Evaluation. The assay condition described in FASN activity assay (*SI Appendix*) was also used for the determination of kinetics parameters. The enzymatic activity of WT dFASN or K813R mutants upon varying concentration of MalCoA was determined at fixed concentrations of NADPH (240 μM) and AcCoA (31 μM). The enzymatic activity of WT dFASN or K813R mutants upon varying concentration of AcCoA was determined at fixed concentrations of NADPH (240 μM) and MalCoA (58 μM). For the kinetics evaluation with AcCoA pre-incubation, AcCoA was added to dFASN proteins to a final concentration of 20 μM. Proteins were then incubated at 37 °C for 1 h, followed by dFASN activity assay. For control groups, dFASN proteins were mixed with 20 μM of AcCoA right before the activity assay without any pre-incubation. Kinetics parameters were calculated by fitting the observed velocities to the Michaelis–Menten equation using GraphPad.

Data, Materials, and Software Availability. All study data are included in the article and/or *SI Appendix*.

ACKNOWLEDGMENTS. We thank the Bloomington *Drosophila* Stock Center (supported by NIH P40OD018537) for the fly stocks that were obtained and used in this study. We thank the *Drosophila* Genomics Resource Center (supported by NIH grant 2P40OD010949) for the cDNA clones obtained and used in this study. We thank FlyBase release (FB2022_02 – March 29th) for data that was obtained and used in this study. We thank BestGene Inc for *Drosophila* embryo injection service. We thank Ross Tomaino from Harvard Medical School Taplin Mass Spectrometry Facility for mass spectrometry analysis. We thank Ann Perera and Lucas Showman from W. M. Keck Metabolomics Research Laboratory of Iowa State University for advice on AcCoA analysis. We thank Baoyu (Stone) Chen and Sheng Yang for the DNA clones and reagents and the help with recombinant protein expression. We thank Justin Walley for advice on mass spectrometry analysis. We thank Basil J. Nikolau and Marna D. Yandeau-Nelson for helpful discussions and advice on enzyme kinetics analysis. We thank the anonymous reviewers for their critically reading of the manuscript and insightful comments and suggestions. Graphical abstract and working model figures were created with BioRender.com. All protein structures were visualized with PyMOL Molecular Graphics System. The protein structure of dFASN was predicted by the I-TASSER server. This work was supported by NIH R01AG058741, NSF CAREER 2046984 to H.B., Glenn/AFAR Scholarships to T.M.

Author affiliations: [a]Department of Genetics, Development, and Cell Biology, Iowa State University, Ames, IA 50011; and [b]Division of Endocrinology, Metabolism and Lipid Research, Department of Medicine, Washington University School of Medicine in St. Louis, St. Louis, MO 63110

1. F. Ameer, L. Scandiuzzi, S. Hasnain, H. Kalbacher, N. Zaidi, De novo lipogenesis in health and disease. *Metabolism* **63**, 895–902 (2014).
2. M. S. Strable, J. M. Ntambi, Genetic control of de novo lipogenesis: Role in diet-induced obesity. *Crit. Rev. Biochem. Mol. Biol.* **45**, 199–214 (2010).
3. J. Lin *et al.*, Hyperlipidemic effects of dietary saturated fats mediated through PGC-1β coactivation of SREBP. *Cell* **120**, 261–273 (2005).
4. Y. Nagai *et al.*, The role of peroxisome proliferator-activated receptor γ coactivator-1 β in the pathogenesis of fructose-induced insulin resistance. *Cell Metab.* **9**, 252–264 (2009).
5. D. B. Savage, Reversal of diet-induced hepatic steatosis and hepatic insulin resistance by antisense oligonucleotide inhibitors of acetyl-CoA carboxylases 1 and 2. *J. Clin. Invest.* **116**, 817–824 (2006).
6. T. M. Loftus, Reduced food intake and body weight in mice treated with fatty acid synthase inhibitors. *Science* **288**, 2379–2381 (2000).
7. M. V. Chakravarthy *et al.*, Inactivation of hypothalamic FAS protects mice from diet-induced obesity and inflammation. *J. Lipid Res.* **50**, 630–640 (2009).
8. X. Xu, J.-S. So, J.-G. Park, A.-H. Lee, Transcriptional control of hepatic lipid metabolism by SREBP and ChREBP. *Semin. Liver Dis.* **33**, 301–311 (2013).
9. G. Liang *et al.*, Diminished hepatic response to fasting/refeeding and liver X receptor agonists in mice with selective deficiency of sterol regulatory element-binding protein-1c. *J. Biol. Chem.* **277**, 9520–9528 (2002).
10. J. D. Horton *et al.*, Combined analysis of oligonucleotide microarray data from transgenic and knockout mice identifies direct SREBP target genes. *Proc. Natl. Acad. Sci. U.S.A.* **100**, 12027–12032 (2003).
11. M. Shamir, Y. Bar-On, R. Phillips, R. Milo, SnapShot: Timescales in cell biology. *Cell* **164**, 1302–1302 (2016).
12. M. Carvalho *et al.*, Effects of diet and development on the *Drosophila* lipidome. *Mol. Syst. Biol.* **8**, 600 (2012).
13. Xue *et al.*, Biochemical membrane lipidomics during drosophila development. *Dev. Cell* **24**, 98–111 (2013).
14. C. Wicker-Thomas *et al.*, Flexible origin of hydrocarbon/pheromone precursors in Drosophila melanogaster [S]. *J. Lipid Res.* **56**, 2094–2101 (2015).
15. C. Heier, R. P. Kühnlein, Triacylglycerol metabolism in *Drosophila melanogaster*. *Genetics* **210**, 1163–1184 (2018).
16. Y. Hu, A. Comjean, N. Perrimon, S. E. Mohr, The Drosophila gene expression tool (DGET) for expression analyses. *BMC Bioinformatics* **18**, 1–9 (2017).
17. J. M. Tennessen *et al.*, Coordinated metabolic transitions during *Drosophila* embryogenesis and the onset of aerobic glycolysis. *G3 (Bethesda)* **4**, 839–850 (2014).
18. I. Ali, R. J. Conrad, E. Verdin, M. Ott, Lysine acetylation goes global: From epigenetics to metabolism and therapeutics. *Chem. Rev.* **118**, 1216–1252 (2018).
19. K. J. Menzies, H. Zhang, E. Katsyuba, J. Auwerx, Protein acetylation in metabolism–metabolites and cofactors. *Nat. Rev. Endocrinol.* **12**, 43 (2016).
20. Q. Wang *et al.*, Acetylation of metabolic enzymes coordinates carbon source utilization and metabolic flux. *Science* **327**, 1004–1007 (2010).
21. S. Zhao *et al.*, Regulation of cellular metabolism by protein lysine acetylation. *Science* **327**, 1000–1004 (2010).
22. E. S. Nakayasu *et al.*, Ancient regulatory role of lysine acetylation in central metabolism. *mBio* **8**, e01894-17 (2017).
23. Q. Jin *et al.*, Fatty acid synthase phosphorylation: A novel therapeutic target in HER2-overexpressing breast cancer cells. *Breast Cancer Res.* **12**, R96 (2010).
24. R. A. Hennigar *et al.*, Characterization of fatty acid synthase in cell lines derived from experimental mammary tumors. *Biochim. Biophys. Acta* **1392**, 85–100 (1998).
25. H.-P. Lin *et al.*, Destabilization of fatty acid synthase by acetylation inhibits de novo lipogenesis and tumor cell growth. *Cancer Res.* **76**, 6924–6936 (2016).
26. S. Smith, The animal fatty acid synthase: One gene, one polypeptide, seven enzymes. *FASEB J.* **8**, 1248–1259 (1994).
27. M. Wu *et al.*, Antidiabetic and antisteatotic effects of the selective fatty acid synthase (FAS) inhibitor platensimycin in mouse models of diabetes. *Proc. Natl. Acad. Sci. U.S.A.* **108**, 5378–5383 (2011).
28. T. S. Angeles, R. L. Hudkins, Recent advances in targeting the fatty acid biosynthetic pathway using fatty acid synthase inhibitors. *Expert Opin. Drug Discov.* **11**, 1187–1199 (2016).
29. S. J. Kridel, W. T. Lowther, C. W. Pemble IV, Fatty acid synthase inhibitors: New directions for oncology. *Expert Opin. Investig. Drugs* **16**, 1817–1829 (2007).
30. V. Sabbisetti *et al.*, p63 promotes cell survival through fatty acid synthase. *PLoS One* **4**, e5877 (2009).
31. A. A. Qureshi, R. A. Jenik, M. Kim, F. A. Lornitzo, J. W. Porter, Separation of two active forms (holo-a and holo-b) of pigeon liver fatty acid synthetase and their interconversion by phosphorylation and dephosphorylation. *Biochem. Biophys. Res. Commun.* **66**, 344–351 (1975).
32. S. M. Najjar *et al.*, Insulin acutely decreases hepatic fatty acid synthase activity. *Cell Metab.* **2**, 43–53 (2005).
33. A. S. Olia *et al.*, Nonenzymatic protein acetylation detected by NAPPA protein arrays. *ACS Chem. Biol.* **10**, 2034–2047 (2015).
34. G. R. Wagner, R. M. Payne, Widespread and enzyme-independent N_ε-acetylation and N_ε-succinylation of proteins in the chemical conditions of the mitochondrial matrix. *J. Biol. Chem.* **288**, 29036–29045 (2013).
35. B. K. Hansen *et al.*, Analysis of human acetylation stoichiometry defines mechanistic constraints on protein regulation. *Nat. Commun.* **10**, 1055 (2019).
36. F. Pietrocola, L. Galluzzi, J. M. Bravo-San Pedro, F. Madeo, G. Kroemer, Acetyl coenzyme A: A central metabolite and second messenger. *Cell Metab.* **21**, 805–821 (2015).
37. L. Shi, B. P. Tu, Acetyl-CoA and the regulation of metabolism: Mechanisms and consequences. *Curr. Opin. Cell Biol.* **33**, 125–131 (2015).
38. R. A. Kulkarni *et al.*, Discovering targets of non-enzymatic acylation by thioester reactivity profiling. *Cell Chem. Biol.* **24**, 231–242 (2017).
39. M. Slaidina, R. Delanoue, S. Gronke, L. Partridge, P. Léopold, A Drosophila insulin-like peptide promotes growth during nonfeeding states. *Dev. Cell* **17**, 874–884 (2009).
40. R. B. Church, F. W. Robertson, Biochemical analysis of genetic differences in the growth of Drosophila. *Genet. Res.* **7**, 383–407 (1966).
41. X.-J. Xie *et al.*, CDK8-cyclin C mediates nutritional regulation of developmental transitions through the ecdysone receptor in Drosophila. *PLoS Biol.* **13**, e1002207 (2015).
42. J. R. Aguila, J. Suszko, A. G. Gibbs, D. K. Hoshizaki, The role of larval fat cells in adult Drosophila melanogaster. *J. Exp. Biol.* **210**, 956–963 (2007).
43. M. Leibundgut, T. Maier, S. Jenni, N. Ban, The multienzyme architecture of eukaryotic fatty acid synthases. *Curr. Opin. Struct. Biol.* **18**, 714–725 (2008).
44. K. Singh *et al.*, Discovery of a regulatory subunit of the yeast fatty acid synthase. *Cell* **180**, 1130–1143.e20 (2020).
45. D. Saggerson, Malonyl-CoA, a key signaling molecule in mammalian cells. *Ann. Rev. Nutr.* **28**, 253–272 (2008).
46. Z. Hu, S. H. Cha, S. Chohnan, M. D. Lane, Hypothalamic malonyl-CoA as a mediator of feeding behavior. *Proc. Natl. Acad. Sci. U.S.A.* **100**, 12624–12629 (2003).
47. T. Narita, B. T. Weinert, C. Choudhary, Functions and mechanisms of non-histone protein acetylation. *Nat. Rev. Mol. Cell Biol.* **20**, 156–174 (2019).
48. T. Baldensperger, M. A. Glomb, Pathways of non-enzymatic lysine acylation. *Front. Cell Dev. Biol.* **9**, 664553 (2021).
49. K. E. Wellen *et al.*, ATP-citrate lyase links cellular metabolism to histone acetylation. *Science* **324**, 1076–1080 (2009).
50. B. W. Wong *et al.*, The role of fatty acid β-oxidation in lymphangiogenesis. *Nature* **542**, 49–54 (2017).
51. S. K. Tiwari, A. G. Toshniwal, S. Mandal, L. Mandal, Fatty acid β-oxidation is required for the differentiation of larval hematopoietic progenitors in Drosophila. *Elife* **9**, e53247 (2020).
52. A. M. James *et al.*, Non-enzymatic N-acetylation of lysine residues by acetylCoA often occurs via a proximal S-acetylated thiol intermediate sensitive to glyoxalase II. *Cell Rep.* **18**, 2105–2112 (2017).
53. A. Rittner, K. S. Paithankar, K. V. Huu, M. Grininger, Characterization of the polyspecific transferase of murine type I fatty acid synthase (FAS) and implications for polyketide synthase (PKS) engineering. *ACS Chem. Biol.* **13**, 723–732 (2018).
54. A. M. James, A. C. Smith, C. L. Smith, A. J. Robinson, M. P. Murphy, Proximal cysteines that enhance lysine N-acetylation of cytosolic proteins in mice are less conserved in longer-living species. *Cell Rep.* **24**, 1445–1455 (2018).
55. S. Y. Roth, J. M. Denu, C. D. Allis, Histone acetyltransferases. *Annu. Rev. Biochem.* **70**, 81–120 (2001).
56. F. Dyda, D. C. Klein, A. B. Hickman, GCN5-related N-acetyltransferases: A structural overview. *Annu. Rev. Biophys. Biomol. Struct.* **29**, 81–103 (2000).
57. E. Wolf *et al.*, Crystal structure of a GCN5-related N-acetyltransferase. *Cell* **94**, 439–449 (1998).
58. L. Wang, L. Liu, S. L. Berger, Critical residues for histone acetylation by Gcn5, functioning in Ada and SAGA complexes, are also required for transcriptional function in vivo. *Genes Dev.* **12**, 640–653 (1998).
59. M.-H. Kuo, J. Zhou, P. Jambeck, M. E. Churchill, C. D. Allis, Histone acetyltransferase activity of yeast Gcn5p is required for the activation of target genes in vivo. *Genes Dev.* **12**, 627–639 (1998).
60. A. K. Walker *et al.*, Conserved role of SIRT1 orthologs in fasting-dependent inhibition of the lipid/cholesterol regulator SREBP. *Genes Dev.* **24**, 1403–1417 (2010).
61. F. Xu *et al.*, Lack of SIRT1 (Mammalian Sirtuin 1) activity leads to liver steatosis in the SIRT1 +/− mice: A role of lipid mobilization and inflammation. *Endocrinology* **151**, 2504–2514 (2010).
62. B. Ponugoti *et al.*, SIRT1 deacetylates and inhibits SREBP-1C activity in regulation of hepatic lipid metabolism. *J. Biol. Chem.* **285**, 33959–33970 (2010).

63. R.-H. Wang, C. Li, C.-X. Deng, Liver steatosis and increased ChREBP expression in mice carrying a liver specific SIRT1 null mutation under a normal feeding condition. *Int. J. Biol. Sci.* **6**, 682–690 (2010), 10.7150/ijbs.6.682.
64. F. Xu *et al.*, Lack of SIRT1 (Mammalian Sirtuin 1) activity leads to liver steatosis in the SIRT1+/− mice: A role of lipid mobilization and inflammation. *Endocrinology* **151**, 2504–2514 (2010).
65. P. Leopold, N. Perrimon, Drosophila and the genetics of the internal milieu. *Nature* **450**, 186–188 (2007).
66. P. W. Hochachka, Intracellular convection, homeostasis and metabolic regulation. *J. Exp. Biol.* **206**, 2001–2009 (2003).
67. C. Lu, C. B. Thompson, Metabolic regulation of epigenetics. *Cell Metab.* **16**, 9–17 (2012).
68. A. Drazic, L. M. Myklebust, R. Ree, T. Arnesen, The world of protein acetylation. *Biochim. Biophys. Acta* **1864**, 1372–1401 (2016).
69. H. Wang, M. V. Airola, K. Reue, How lipid droplets "TAG" along: Glycerolipid synthetic enzymes and lipid storage. *Biochim. Biophys. Acta Mol. Cell Biol. Lipids* **1862**, 1131–1145 (2017).
70. B. N. Sheikh, A. Akhtar, The many lives of KATs – detectors, integrators and modulators of the cellular environment. *Nat. Rev. Genet.* **20**, 7–23 (2019).
71. M. Doi, J. Hirayama, P. Sassone-Corsi, Circadian regulator CLOCK Is a histone acetyltransferase. *Cell* **125**, 497–508 (2006).
72. D. Ivanov *et al.*, Eco1 is a novel acetyltransferase that can acetylate proteins involved in cohesion. *Curr. Biol.* **12**, 323–328 (2002).
73. L. Carlisle-Moore, C. R. Gordon, C. A. Machutta, W. T. Miller, P. J. Tonge, Substrate recognition by the human fatty-acid synthase. *J. Biol. Chem.* **280**, 42612–42618 (2005).
74. A. Rittner, K. S. Paithankar, A. Himmler, M. Grininger, Type I fatty acid synthase trapped in the octanoyl-bound state. *Protein Sci.* **29**, 589–605 (2020).